Water Supply

Water Supply Vol 22 No 4, 4639 doi: 10.2166/ws.2022.123

The hydraulic investigation of inflatable weirs

S. Behnam Sarvarinezhad[a], Mahmoud Bina[b], Ehsan Afaridegan[c,*], Abbas Parsaie[b] and Fatemeh Avazpour[c]

[a] Department of Water Engineering, Faculty of Agriculture, Isfahan (Khorasgan) Branch, Islamic Azad University, Isfahan, Iran
[b] Faculty of Water and Environmental Engineering, Shahid Chamran University of Ahvaz, Ahvaz, Iran
[c] Department of Civil Engineering, Faculty of Engineering, Yazd University, Yazd, Iran
*Corresponding author. E-mail: Ehsan.Afaridegan@stu.yazd.ac.ir

EA, 0000-0001-5492-598X

ABSTRACT

In this research, the models of Inflatable weirs with internal pressures of 0.5 and 1.4 at three heights of 0.15, 0.2 and 0.25 m were constructed. The deflectors were used in two geometric sections, including rectangular and triangular shapes, and they were installed at angles of 30, 45, and 60 degrees downstream of the weir body. The results showed that the value of the C_d changes between 0.28 and 0.35 while the range of the ratio of the upstream flow head on the crest to the radius of the downstream side of the inflatable weir (h_V/R) varies between 0.2 and 1.5. The flow by crossing over the inflatable weir and colliding with the surface of the downstream stilling basin loses its energy by about 10–85%. The relative horizontal distance of the projectile-jet from the crest (L_{impact}/R) varies between 1.6 and 2.8. The effect of the deflector on the C_d is negligible due to being located in the supercritical part of the weir. Examination of the obtained results declared that the deflector has a considerable effect on energy dissipation.

Key words: deflector, discharge coefficient, energy dissipation, flow measurement, inflatable weir

HIGHLIGHTS

- The hydraulic properties of the Inflatable weir, including discharge coefficient (Cd), the flow energy dissipation ratio (EDR), and the profile of the outlet jet of the deflector were investigated.
- The stage-discharge relation (rating curve) of inflatable weirs was provided.
- The effects of defector and its installation angle on the properties of outlet jet and energy dissipation have been investigated.

NOTATION

The following symbols are used in this paper:

C_d	discharge coefficient;
d_{crest}	flow depth above the weir crest;
d_0	jet thickness;
d_{C1}	critical depth at the upstream of the weir;
d_{C2}	critical depth over the weir crest;
Fr	Froude number;
g	acceleration due to the gravity;
H_{dwn}	total head at the downstream of the weir;
H_{up}	total head at the upstream of the weir;
h	deflector height;
h_S	flow depth over the weir crest;
h_V	total head over the weir crest;
L_{impact}	length of the projectile-jet;
P	weir height;
P_i	the internal pressure of the weir;
q	discharge per unit width;
R	radius of curvature of inflatable weir;
Re	Reynolds numbers;

u streamwise velocity component;
V flow velocity at the upstream of the weir;
V_0 projected jet velocity;
V_1 flow velocity at the downstream of the weir;
We Weber numbers;
x longitudinal distance from the origin of the coordinates;
y transverse distance from the origin of the coordinates;
Y_0 flow depth at the upstream of the weir;
y_1 downstream flow depth;
y_2 sequence depth;
α internal pressure coefficient;
θ angular of the deflector's shape;
θ_0 deflected jet angle;
μ fluid viscosity;
ρ fluid density;
σ surface tension; and
ϕ_{def} angular position of the deflector on the body of the weir.

1. INTRODUCTION

Inflatable weirs are popular solutions for any engineering and environmental problems, such as irrigation, power generation, flood control and environmental improvement (Zheng *et al.* 2021). Inflatable weirs, also known as rubber dams, are flexible elliptical structures made of rubberized material attached to a concrete foundation and inflated by air, water, or a combination of them (Kumar & ul Islam 2019). In recent years, using rubber dams in developing countries has substantially grown due to the more durable rubber membrane (Saleh & Mondal 2001). Inflatable weirs can be deflated if not needed and inflated again in flood situations with water or air. These are relatively easy to install, do not corrode, and require less maintenance than other weirs. Therefore, it can be said that the construction of this type of weir is more cost-effective (or economical) than small dams (Anwar 1967). Also, these kinds of weirs have a higher discharge than broad and sharp-crested weirs for the given upstream head (Chanson 1997). Due to the ease of construction, implementation, and operation, using inflatable weirs is increasing (Cheraghi-Shirazi *et al.* 2014). Implementation of this type of weir requires the study of their hydraulic behavior based on fluid-structure interaction. In fact, more accurate understanding about the hydraulic behavior of this structure located in the flow path is important to increase the efficiency of this type of structure. According to the relationship between the flow head and the discharge overflow the weir, the discharge relationship in the inflatable weir is defined as (Anwar 1967).

$$q = C_d\sqrt{2g}h_V^{1.5} \tag{1}$$

where q is the discharge per unit width; C_d is the discharge coefficient; h_v is the total head on the crest as shown in Figure 1; and g is acceleration due to gravity.

Anwar (1967) performed extensive studies about inflatable weirs and presented a discharge coefficient equation for them. He found that generally the discharge coefficient (C_d) depends on the ratio (h_V/P) and for different kinds of inflatable weirs, it varies as this ratio changed. Al-Shami (1983) experimentally investigated the C_d of inflatable weirs. He presented two separate equations to calculate the C_d of inflatable weirs inflated by air and water. Chanson (1997) mentioned that the nappe adherence at the downstream of the rubber dam may lead to instability of the flow and failure of the dam. Chanson (1998) studied the hydraulics of inflatable weirs in two ways, with and without a deflector. He found that to have an effective deflector with an excellent operation, it is necessary to aerate the lower layer of flow by aerator systems installed at the deflector position. The length of the water projectile (L_{impact}) is also calculated by studying the hydraulics of the flow over the inflatable weir, with and without a deflector. The nappe trajectory and wall pressure distribution of circular inflatable dams with deflectors was analyzed and it was found that the adherence pressure is reduced due to the operation of deflectors and they can avoid the dams' instability. Alhamati *et al.* (2005a) determined the C_d of inflatable weirs designed at different internal pressures. Their experimental data were combined with the results of Anwar (1967), finally, they provided equations mentioned in the next sections to calculate the discharge coefficient. They declared that C_d increases by increasing (h_V/P). Cheraghi-Shirazi *et al.* (2014) showed that the hydraulic flow characteristics over the equilibrium shape of the flexible rubber dam are similar to those of the rigid circular-crested weirs.

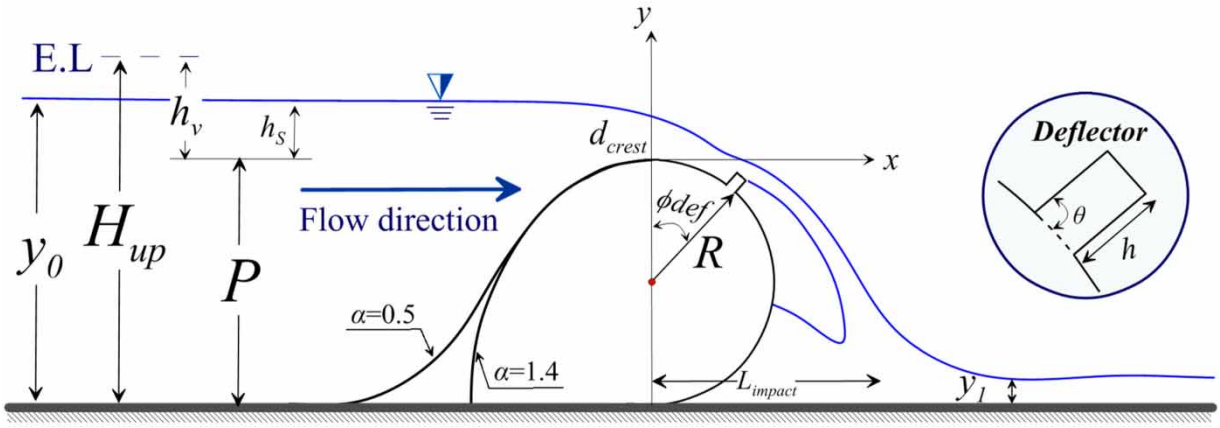

Figure 1 | Geometric and hydraulic characteristics of the inflatable weir.

In this study, the discharge coefficient, three potential of the weir in energy dissipation, suitable shape and location of deflector and its effects on projectile-jet length are investigated. To this aim, inflatable weirs with minimum and maximum internal pressure, in a fully upright position, are studied. Two different shapes of deflectors, rectangular and triangular, are installed at 3 different angular positions of the weir's body. The study of inflatable weir in fully standing conditions by considering the shape of the real upstream curve of the weir and using the triangular and rectangular shape for deflector are the innovations of the present study. Also, in this research, the results obtained for the discharge coefficient and also the length of the water projectile are compared with the results presented by previous researchers for a circular-crested weir and inflatable weir (Table 1).

2. MATERIALS AND METHODS

2.1. Dimensional analysis

A mathematical relationship can be developed between the affective variables on hydraulic flow of the inflatable weir by using dimensional analysis. Hydraulic and geometric parameters affecting the C_d and relative L_{impact} of these weirs are shown in Figure 1. According to this figure, the main parameters affecting the hydraulic properties of the inflatable weir (C_d and L_{impact}) are given in Equation (2):

$$\left[\frac{L_{\text{impact}}}{R}, C_d\right] = f(h_V, R, V, g, \rho, \phi_{def}, \alpha, \theta, \sigma, \mu) \tag{2}$$

where R is the radius of the downstream part of the body of the weir ($R = P/2$); V is the flow velocity at upstream; ρ is density of the fluid; σ is the water surface tension; μ is the water viscosity; ϕ_{def} is the angular position of the deflector; α is the internal pressure coefficient; θ is the deflector angle; and L_{impact} is the length of the projectile-jet. Using the Buckingham Π-theorem, the involved dimensionless parameters in the C_d and the L_{impact} of the flow are derived as described in Equation (3). Three parameters: V, ρ, and R are considered as repetitive parameters to perform the dimensional analysis:

$$\left[\frac{L_{\text{impact}}}{R}, C_d\right] = f\left(\frac{h_V}{R}, \phi_{def}, \alpha, \theta, \text{Fr}, \text{We}, \text{Re}\right) \tag{3}$$

where h_V/R is the ratio of upstream head over the crest to its radius, Fr, We, and Re are the Froude, Weber, and Reynolds numbers, respectively. The depth of flow was kept at more than 3 cm during the laboratory test to remove the effect of surface tension. There is a fully turbulent and sub-critical flow upstream of the weir, so the effects of Reynolds and Froude number could be ignored. According to the points mentioned above, Equation (3) can be written as Equation (4):

$$\left[\frac{L_{\text{impact}}}{R}, C_d\right] = f\left(\frac{h_V}{R}, \phi_{def}, \alpha, \theta\right) \tag{4}$$

Table 1 | Discharge coefficients for the circular-crested and inflatable weirs and analytical solution of trajectory jet length proposed in different studies

Reference	C_d – Circular crested weir	Comments
Fawer (1937)	$1 + 0.221\left(\frac{h_v}{R}\right) - 0.026\left(\frac{h_v}{R}\right)^2$	$0.5 < \frac{h_v}{R} < 3$
Chanson & Montes (1998)	$1.2676\left(\frac{h_v}{R}\right)^{0.1811}$	Partially-developed inflow $0.35 < \frac{h_v}{R} < 3.5$
	$1.1854\left(\frac{h_v}{R}\right)^{0.1358}$	Fully-developed inflow $0.45 < \frac{h_v}{R} < 1.9$
Bagheri & Kabiri-Samani (2020)	$1.22\left(\frac{h_S}{2R}\right)^{0.2}$	$\frac{h_S}{R} \leq 2$
	C_d – Inflatable weir	
Anwar (1967)	$0.361 + 0.188\left(\frac{h_v}{P}\right)$	$0.2 \leq \frac{h_v}{P} \leq 0.7$
Al-Shami (1983)	$0.4866\left(\frac{h_v}{P}\right)^{0.11}$	Inflated with air $0.05 \leq \frac{h_v}{P} \leq 0.17$
	$0.4338\left(\frac{h_v}{P}\right)^{0.0694}$	Inflated with water $0.045 \leq \frac{h_v}{P} \leq 0.31$
Alhamati *et al.* (2005a)	$0.5066\left(\frac{h_v}{P}\right)^{0.2447}$	$0.04 \leq \frac{h_v}{P} \leq 0.3$
Chanson (1998)	L_{impact}/R $\left(1+\frac{h}{R}\right)\sin\phi_{def} + \text{Fr}_0^2\cos(\phi_{def}-\theta_0)\times$ $\left(\sqrt{(\sin(\phi_{def}-\theta_0))^2 + \frac{2}{\text{Fr}_0^2}\left(\frac{D}{R}-1+(1+\frac{h}{R})\cos\phi_{def}\right)} - \sin(\phi_{def}-\theta_0)\right)$	Analytical solution
	$\text{Fr}_0 = \sqrt{\frac{V_0^2}{g.R}}$	
	$\theta_0 = \theta\sqrt{\tanh\left(\frac{h}{d_0.\theta}\right)}$	

The stage-discharge relationship for an inflatable weir can be expressed by the following functional relationship:

$$0 = \varphi(h_S, R, q, g, \rho, \sigma, \mu) \tag{5}$$

The following functional relationship can be deduced by using the Π-theorem of dimensional analysis:

$$f\left(\frac{d_{C1}}{R}, \frac{h_S}{R}, \text{Re}, \text{We}\right) = 0 \tag{6}$$

where dc is the critical depth $\left(d_{C1} = q^{2/3}/g^{1/3}\right)$. According to the description in the previous section, finally, Equation (6) is rewritten as follows:

$$\frac{d_{C1}}{R} = f\left(\frac{h_S}{R}\right) \tag{7}$$

Other objectives of the present study are examining the amount of energy dissipation in different geometric conditions of the weir and installing the deflectors. To examine the amount of energy dissipation, the effected parameters are given in Equation (8):

$$\mathrm{EDR} = \frac{\Delta H}{H_{up}} = f(R, h_V, V, g, \rho, \phi_{def}, \alpha, \theta, \mu, \sigma) \tag{8}$$

$$\Delta H = H_{up} - H_{dwn} \tag{9}$$

where H_{up} is the upstream total energy and H_{dwn} is the downstream total energy (Parsaie & Haghiabi 2019). According to the explanations mentioned above and using the Π-theorem, the dimensionless parameters affected on energy dissipation in inflatable weirs are as Equation (10):

$$\mathrm{EDR} = \frac{\Delta H}{H_{up}} = f\left(\frac{d_{C2}}{R}, \phi_{def}, \alpha, \theta\right) \tag{10}$$

where d_{C2} is the critical depth on the crest of the weir.

2.2. Experimental model

Experiments were conducted in a flume with glass walls and a metal bed with a length of 11.9 m, depth of 0.5 m, and width of 0.25 m. The inflow is supplied with a pump. A special valve is used to adjust the discharge of inflow. The discharge was measured by a 53° triangular weir with an accuracy measurement of 1%, located at the end of the flume (Figure 2). A point gauge with 1 mm accuracy was used to record the water surface level, and a Micro Moline with the propeller's diameter of 20 mm giving an accurate measurement of ± 0.01 m/s was used to collect longitudinal velocity data. It should be noted that the data collected for this study were not complicated and the devices used to collect the required data are in the good quality category. Figure 3 shows a model of the inflatable weir tested in the laboratory.

According to Anwar (1967), the downstream curve of the weir (from the crest to downstream) is semicircular and the upstream curve of the weir's body (from the axis of the crest to upstream) is proportional to α, which is defined as:

$$\alpha = \frac{P_i}{P} \tag{11}$$

where P_i is the internal pressure of the weir and P is the weir's height. In this study, we considered the inflatable weir by considering the minimum (0.5) and maximum (1.4) amount for α when both are at standing position. Anwar's equation to

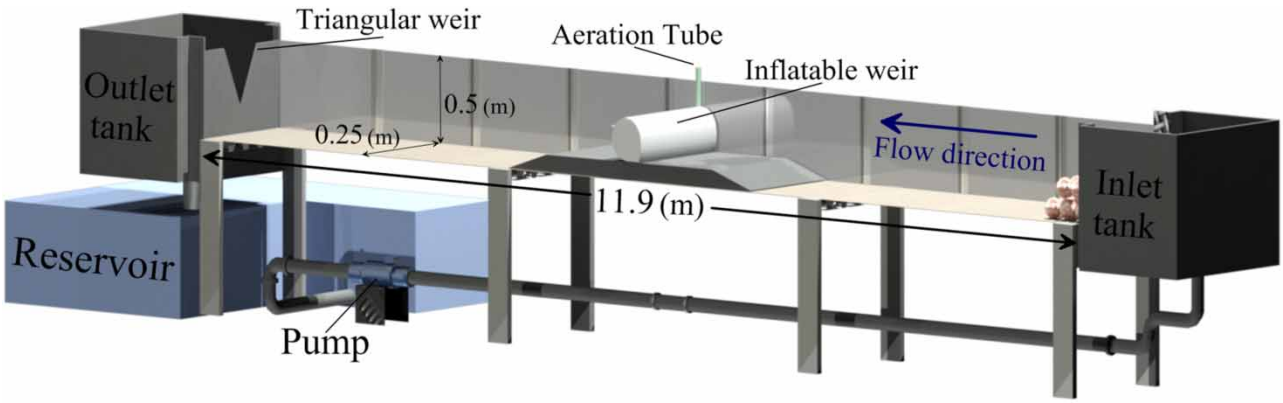

Figure 2 | Schematic of the laboratory flume used.

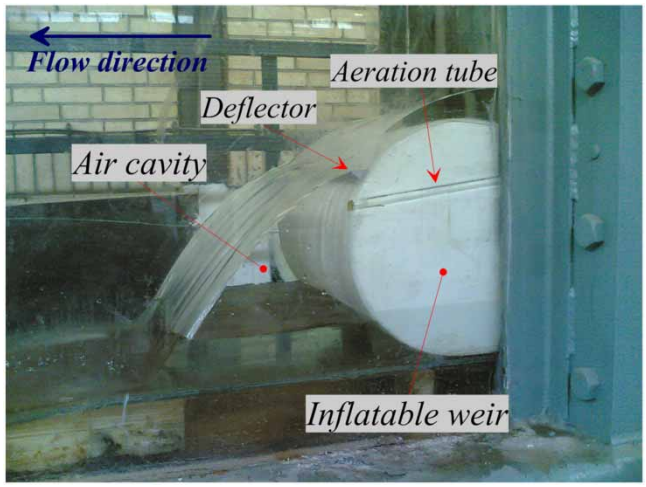

Figure 3 | Details of the inflatable weir.

determine the upstream curve of the inflatable weir's body is as follows (Anwar 1967):

$$\xi = \sqrt{\frac{\alpha}{2}} \int_{Arccos\left(\frac{\eta}{\alpha}-1\right)}^{\pi} \left[\frac{1-\alpha(\sin\theta)^2}{\sqrt{1-\frac{\alpha}{2}(\sin\phi)^2}} \right] d\phi \tag{12}$$

$$\xi = \frac{x}{P} \tag{13}$$

$$\eta = \frac{y}{P} \tag{14}$$

where x is the longitudinal distance from the origin of the coordinates and y is the transverse distance from the origin of the coordinates. As mentioned, by using the values of 0.5 and 1.4 for α and considering the three heights of 25, 20, and 15 cm ($P = 15$, 20, and 25 cm) for the weir, the equation of the upstream curve of the body was determined. Poplar wood was used to make the desired models. The deflectors were also made in two shapes, triangular ($\theta = 45°$) and square ($\theta = 90°$) with a ratio of $h/P = 0.15$ using Tooka wood and studied at three angles of $\phi_{def} = 30$, 45, and 60° on the body of the weir. All models were insulated against water penetration.

One of the effective ways to make flow stable is aeration near the downstream body of the inflatable weir. The air under the water jet will be gradually evacuated and enter the downstream flow. Due to the air evacuation, the water jet is inclined towards the weir body of the weir and the flow sticks to the body over time, consequently, the projectile jet will disappear. The vibration of the weir and flow instability are the most important consequences of eliminating the projectile jet. Therefore, in order to prevent flow instability, some rubber tubes were also placed in the groove on the model and on the flume walls simultaneously for aeration. Figure 4 shows the aeration equipment and the position of the aeration tube on the weir's body.

The geometric characteristics of the models and the planning of the experiments are given in Table 2. The discharge of flow changed between 1 and 20 L/s in all experiments. The flow head on the weir's crest ranges from 3 to 12 cm. The walls of the flume cause some surface waves. Due to the low rate of velocity in the selected test range, the range of effect of the waves is very small and the effect of sidewall friction on the flow is negligible in a narrow flume.

3. RESULTS AND DISCUSSION

In this section, the results obtained from the experiments are presented and analyzed. Initially, the water surface profile (WSP) over the inflatable weir at the different discharges is shown in Figure 5. The smooth passage of the flow without any disturbance over the body is an essential point to consider. The disturbance and fluctuations of the flow increase the energy loss, which in turn reduces the hydraulic efficiency (discharge capacity) and causes erroneous measurement of

Figure 4 | Aeration equipment and placement position of the aeration tube on the body of the weir.

Table 2 | Geometric characteristics of models and sequence of experiments

Num (–)	P (m)	α (–)	ϕ_{def} (°)	θ (°)	Num (–)	P (m)	α (–)	ϕ_{def} (°)	θ (°)
1	0.15	0.5	30	90	16	0.15	0.5	30	45
2	0.15	0.5	45	90	17	0.15	0.5	45	45
3	0.15	0.5	60	90	18	0.15	0.5	60	45
4	0.2	0.5	30	90	19	0.2	0.5	30	45
5	0.2	0.5	45	90	20	0.2	0.5	45	45
6	0.2	0.5	60	90	21	0.2	0.5	60	45
7	0.15	1.4	30	90	22	0.15	1.4	30	45
8	0.15	1.4	45	90	23	0.15	1.4	45	45
9	0.15	1.4	60	90	24	0.15	1.4	60	45
10	0.2	1.4	30	90	25	0.2	1.4	30	45
11	0.2	1.4	45	90	26	0.2	1.4	45	45
12	0.2	1.4	60	90	27	0.2	1.4	60	45
13	0.25	1.4	30	90	28	0.25	1.4	30	45
14	0.25	1.4	45	90	29	0.25	1.4	45	45
15	0.25	1.4	60	90	30	0.25	1.4	60	45

flow discharge. According to the experimental results and WSP in Figure 5, in all discharges, the water surface over the inflatable weir is smooth and regular and there is no disturbance or fluctuation. Hence, the flow measurement by this structure can be performed easily.

As it is clear from Equation (1), the flow depth is directly dependent on the flow rate so as it increases, Q will be increased. The upstream water surface is uniform and by passing over the weir and leaving the deflector, it is thrown away from the weir body in the form of a jet. For proper operation of inflatable weirs, aeration (under outlet-jet leaving the deflector) is essential. In the experiments, it was observed that if the aeration is not performed well, the outlet jet downstream of the weir disappeared and stuck to the weir body. Figure 6 shows the aeration details.

As the flow passes over the downstream circular side of the weir, momentum is transferred between the fluid and the air trapped between the fluid and the weir body. The momentum transfer accelerates the air, and due to preventing the weir body

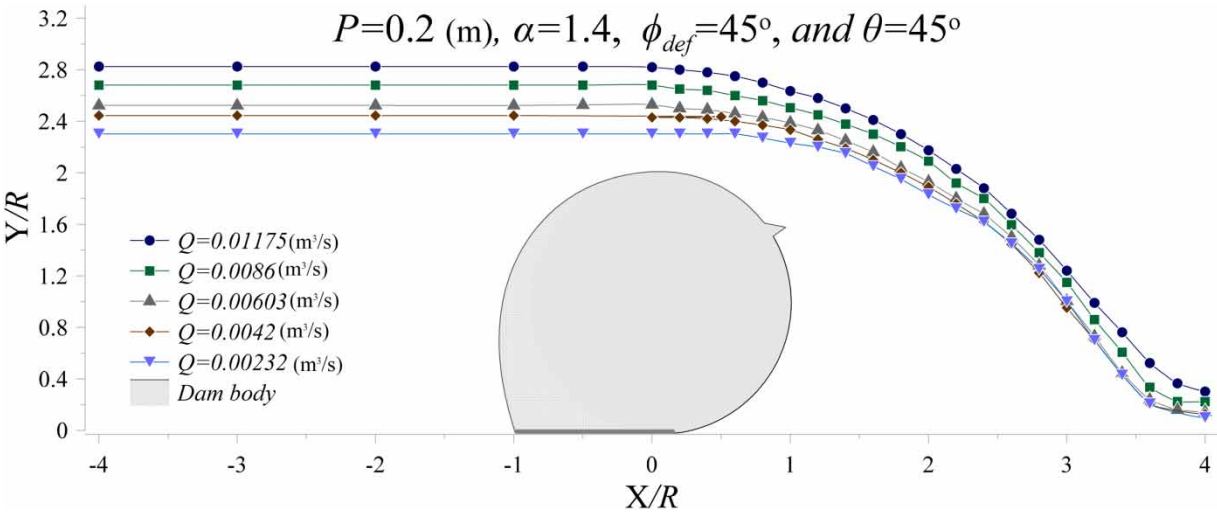

Figure 5 | Water surface profiles (WSPs) along the inflatable weir.

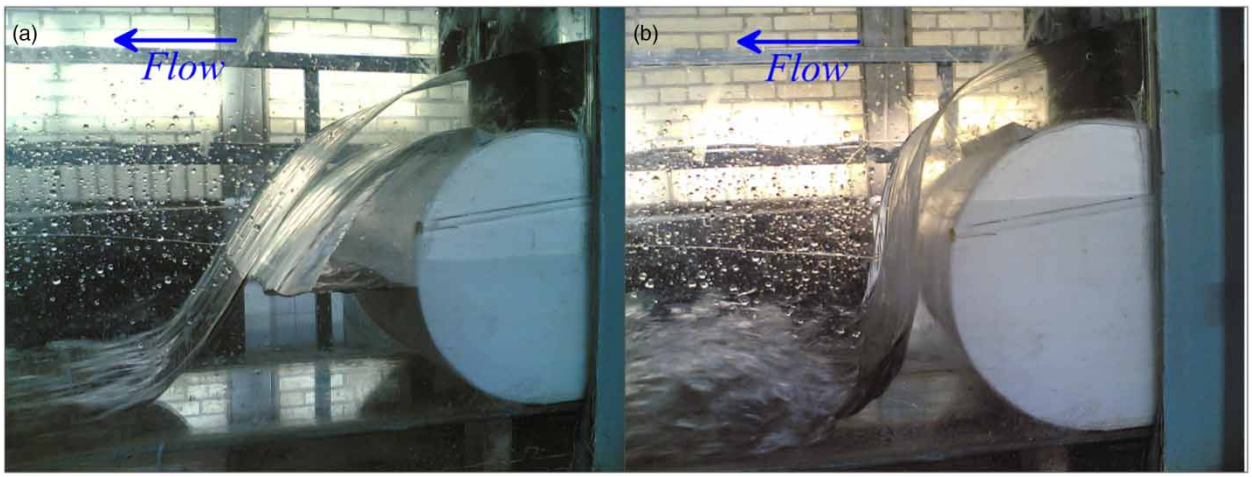

Figure 6 | Overflow of inflatable weir: (a) with aeration; (b) without aeration.

from aeration, the pressure under the outlet-jet decreases, hence the outlet-jet adheres to the weir body. Adhesion of the outlet jet to the downstream part of the weir negatively affects the hydraulic performance of the inflatable weir.

3.1. Stage-discharge relation

The stage-discharge relation (rating curve) of any flow measuring structure, especially in weirs (or small dams), is an important factor for the selection and design of such structures in water engineering projects.

Having the rating curve and measuring the water level in the dam's reservoir (upstream of the dam), the outlet flow is easily estimated. For this purpose, the rating curve for inflatable weirs as shown in Figure 7 was prepared based on the values measured in the laboratory. The values of d_{C1}/R versus the dimensionless flow depth upstream of the weir crest (h_S/R) are plotted in Figure 7.

The stage-discharge equation of flow measurement structure such as a weir is expressed as a power relationship such as $d_{C1}/R = a(h_s/R)^m$, a and m are numerical constants that should be determined experimentally (Bijankhan & Ferro 2017). Considering this, a power function was fitted on the dataset presented in Figure 7. The mathematical formula as described in Equation (15) is obtained for the stage-discharge relation. Another proposed relationship is presented in Equation (16)

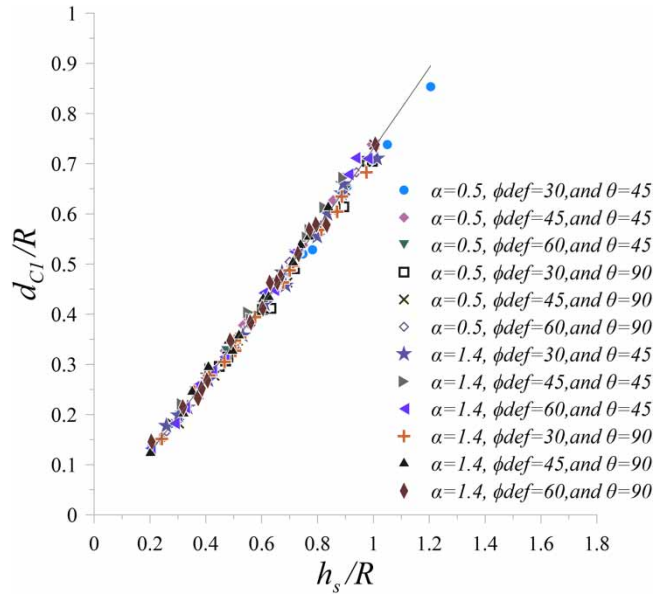

Figure 7 | Dimensionless values of the critical depth (d_{C1}/R) versus the dimensionless flow depth upstream of the weir crest (h_s/R).

with R-squared correlation (R^2) and mean relative error percentage (Equation (17)):

$$\left[\frac{d_{C1}}{R}\right] = 0.73\left(\frac{h_s}{R}\right)^{1.09} \quad (15)$$
$$R^2 = 0.9943$$
$$\text{ARE } (\%) = 2.51$$

$$\left[\frac{d_{C1}}{R}\right] = 0.75\left(\frac{h_s}{R}\right) - 0.032 \quad (16)$$
$$R^2 = 0.994$$
$$\text{ARE } (\%) = 2.74$$

$$\text{ARE } (\%) = \frac{\sum_{i=1}^{i=N}\left(\frac{\text{abs}(f_i - O_i)}{f_i} \times 100\right)}{N} \quad (17)$$

where f is the observed value, O is the calculated value by equation, and N is the total number of data. As it is clear from the relations and their accuracy, the stage-discharge relationship in the form of power relationship (Equation (15)) and linear relationship (Equation (16)) have good accuracy.

If aeration is not performed and consequently nappe is eliminated, the flow head will increase at a constant flow rate at the upstream. Also, the slope of the stage-discharge curve will decrease.

Figure 8 shows a comparison of the stage-discharge relation in the inflatable, circular-crested weir (Ramamurthy & Vo 1993), and broad-crested weir (Hager & Schwalt 1994). According to this diagram, for a given value of h_S/R, the amount of d_{C1}/R in a circular-crested weir is more than the other two cases and the lowest amount of d_{C1}/R occurred in a broad-crested weir.

3.2. Discharge coefficient

One of the important goals of this research is the development of a mathematical equation for the discharge coefficient C_d of the inflatable weir. The most important and effective parameter in determining the C_d is the relative upstream head (h_V/R). In Figure 9 the values of the C_d versus h_V/R are plotted for all experiments in this study.

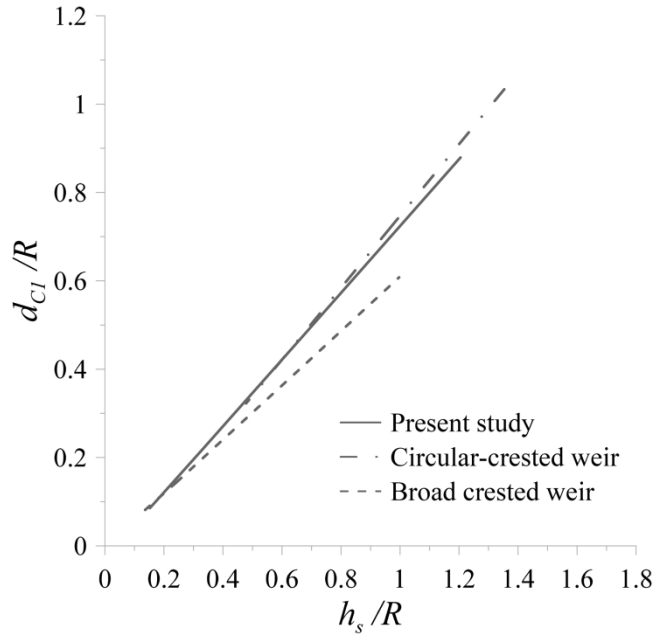

Figure 8 | Stage–discharge relation of the inflatable weir, circular crested weir, and broad-crested weir.

As shown in this figure, the C_d changes between 0.28 and 0.35 for the inflatable weir and 0.37 and 0.48 for the circular crested weir while the range of h_V/R varies between 0.2 and 1.5. The overlap of the points in Figure 9 shows that the three parameters of the take-off of outlet-jet of the deflector (θ), the angular position of the deflector (ϕ_{def}) and the internal pressure coefficient (α) do not have significant effects on the C_d. When the flow passes over the crest and is crossing the critical point, it enters the supercritical zone where the deflector is located. In the supercritical flow, the control point is at the upstream. In this flow condition, the flow characteristics are not transmitted upstream and all the effects received are due to the information sent from the upstream to the downstream. The location of the deflector in the supercritical flow zone is the reason that the two geometric parameters of the deflector (i.e. and θ) can not affect the C_d. Internal pressure α of the inflatable weir also does not affect the C_d. This point is also presented in the results of Alhamati *et al.* (2005b). The greatest effect of the

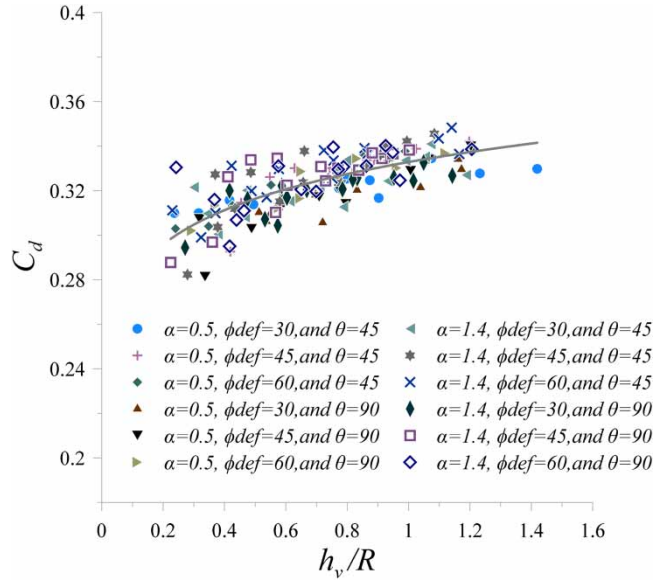

Figure 9 | Values of C_d versus the h_v/R of the inflatable weirs.

internal pressure ratio (α) is on the formation of the longitudinal cross-section of the inflatable weir. The upstream flow of the inflatable weir is always subcritical and as a result, the values of the Fr number are very small and its effect can be ignored. In this study, to provide a suitable mathematical formula for the C_d, different functions were fitted to the points of Figure 9, and finally, Equation (18) was founded with the lowest error:

$$C_d = 0.167 + 0.1657\left(\frac{h_V}{R}\right)^{0.153} \tag{18}$$

As is shown in Figure 10, the relation of the flow head and the depth is linear. So, to estimate the C_d (Equation (18)), if the flow depth is used instead of the flow head, the value of error can be dissembled.

Figure 11 is the longitudinal velocity profiles taken at crests of the inflatable weirs at maximum discharge (Q = 20 L/s). As can be seen, the velocity profiles on the inflatable weir crests from the highest value at minimum depth to the lowest value at

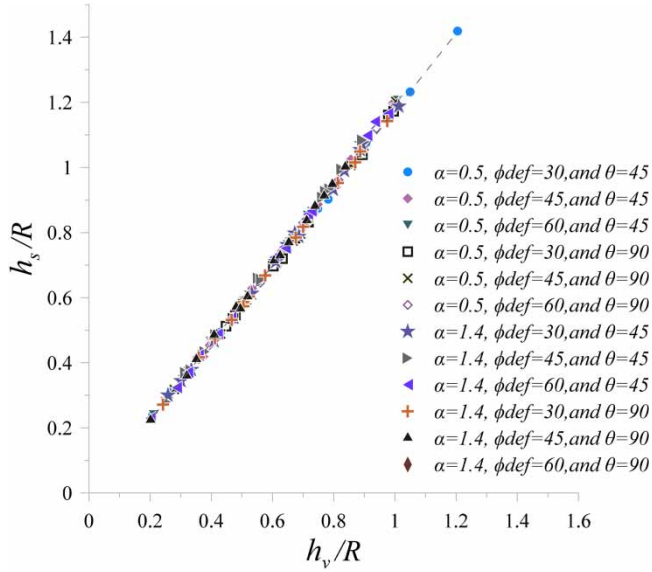

Figure 10 | Dimensionless values of the upstream total head (h_V/R) versus the dimensionless values of the upstream flow depth (h_s/R) on the crest.

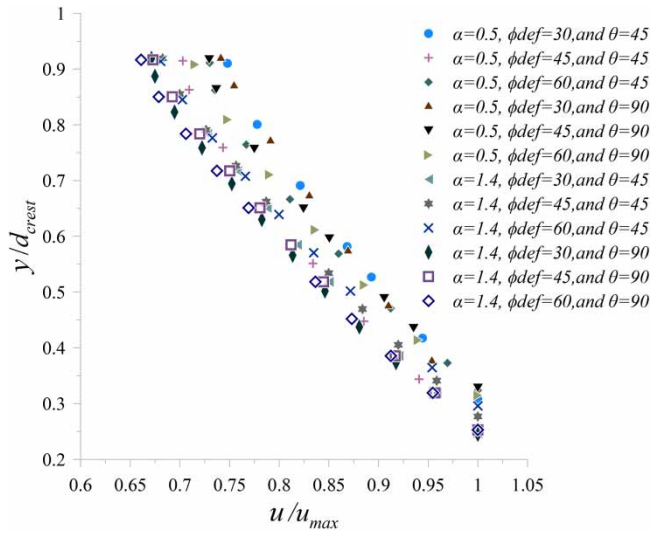

Figure 11 | Dimensionless Longitude velocity (u/u_{max}) profile on the crest.

the water surface are in the form of a nonlinear curve. The study of longitudinal velocity is also showing that the θ and ϕ_{def} do not have any significant effect on the velocity profile. The velocity is highest near the crest of the weir and by decreasing this distance from the crest and moving towards the water surface, the velocity decreases. The intensity of deceasing is decreased because of the presence of air friction.

3.3. Energy dissipation

The structural design of the downstream stilling basin requires the determination of the amount of pressure and hydrodynamic force that the falling jet exerts on its concrete slab. Therefore, determining the amount of energy dissipation is one of the most important issues in the study of dams and weirs. When the flow-jet leaves the deflector, a small amount of its energy is lost due to air resistance (flow-air interaction) and a significant amount of its energy is lost due to collision with the surface of the downstream stilling basin. Examination of laboratory data was performed to determine energy dissipation, the results of which are shown in Figure 12. In this figure, the range of changes in energy dissipation, and a ± 20 confidence interval is specified.

By increasing Q, a layer of water is created on the floor of the stilling basin (water blanket) which reduces the intensity of the collision of falling jet to the surface of the concrete slab, thus EDR reduces. As Q increases, the thickness of this layer increases, thus the turbulence caused by the collision falling jet with the floor reduces more. Therefore, less amount of energy is dissipated. On the other hand, because the increasing of Q and the increasing of kinetic energy of flow-jet are not in the same ratio, hence, the velocity and kinetic energy of the outlet jet decreases, as a result, the spreading of the falling-jet is decreased, therefore, the thickness of the falling-jet and water blanket increases. Figure 12 shows that this structure can dissipate the flow energy between 10 and 85% in the relative upstream head (d_{C2}/R) ranges from 0.1 to 0.7. According to the flow pattern around the deflectors, a vortex is formed in front of the rectangular deflector that causes energy dissipation. Due to the lack of formation of this vortex in the triangular deflector, less EDR occurs and as a result, the horizontal length of the projectile-jet increases. As the length of the projectile-jet increases, the spreading of the flow jet increases, which in turn reduces the thickness of the layer of water blanket and its effect on reducing the turbulence of the collision is reduced, therefore, the EDR increases. The results show that increasing the d_{C2}/R (increasing the flow discharge at a constant weir's height) reduces the EDR (%). The weir's height, the geometric shape of the deflector, and its location affect the amount of EDR. By increasing the weir's height at different angles of deflectors, the amount of EDR increases. Also, in each model, the amount of EDR is directly related to the deflector angle. The maximum amount of EDR was obtained at 60° and the lowest value of EDR was obtained at 30°. Results show that in the presence of a rectangular deflector, the flow energy has a greater energy

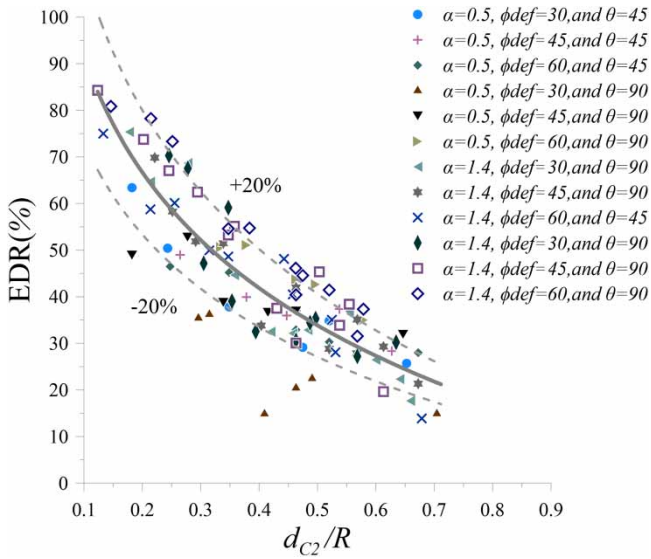

Figure 12 | Values of the flow energy dissipation ratio (EDR(%)) in the inflatable weir versus the dimensionless values of critical depth on the crest (d_{C2}/R).

reduction than a triangular deflector. Finally, a mathematical formula for EDR is developed as Equation (19):

$$\mathrm{EDR}(\%) = \left(0.95 - 0.94\left(\frac{d_{C2}}{R}\right)^{0.85} - 4.85(\phi_{\mathrm{def}})^{-1.37} - 4.2(\theta)^{-1.5}\right) \times 100 \tag{19}$$

where θ and ϕ_{def} is in degrees.

The flow condition at section 1 (in which the depth is shown with y_1) is sub-critical. Then the flow arrived at section 2 (which the depth is shown with y_2) by creating a hydraulic jump. The amount of energy in section 2 is significantly reduced compared to section 1 due to the hydraulic jump and hydraulic jump conditions. Figure 13 shows the energy dissipation data of an inflatable weir and circular weir (Chanson & Montes 1998) and drop structure (Rand 1955).

According to Figure 13, the amount of energy dissipation in an inflatable weir is more than in a circular-crested weir and the drop structure. The presence of a deflector in the stream flow path causes the deflector to act as an obstacle and the flow energy will be decreased due to their collision. On the other hand, the presence of a deflector prevents sticking of the flow to the downstream part of the body of the weir, so the downstream part of the weir acts as a drop. Consequently, energy dissipation in inflatable weirs with deflector is significant compared to the circular-crested wires and drop structures.

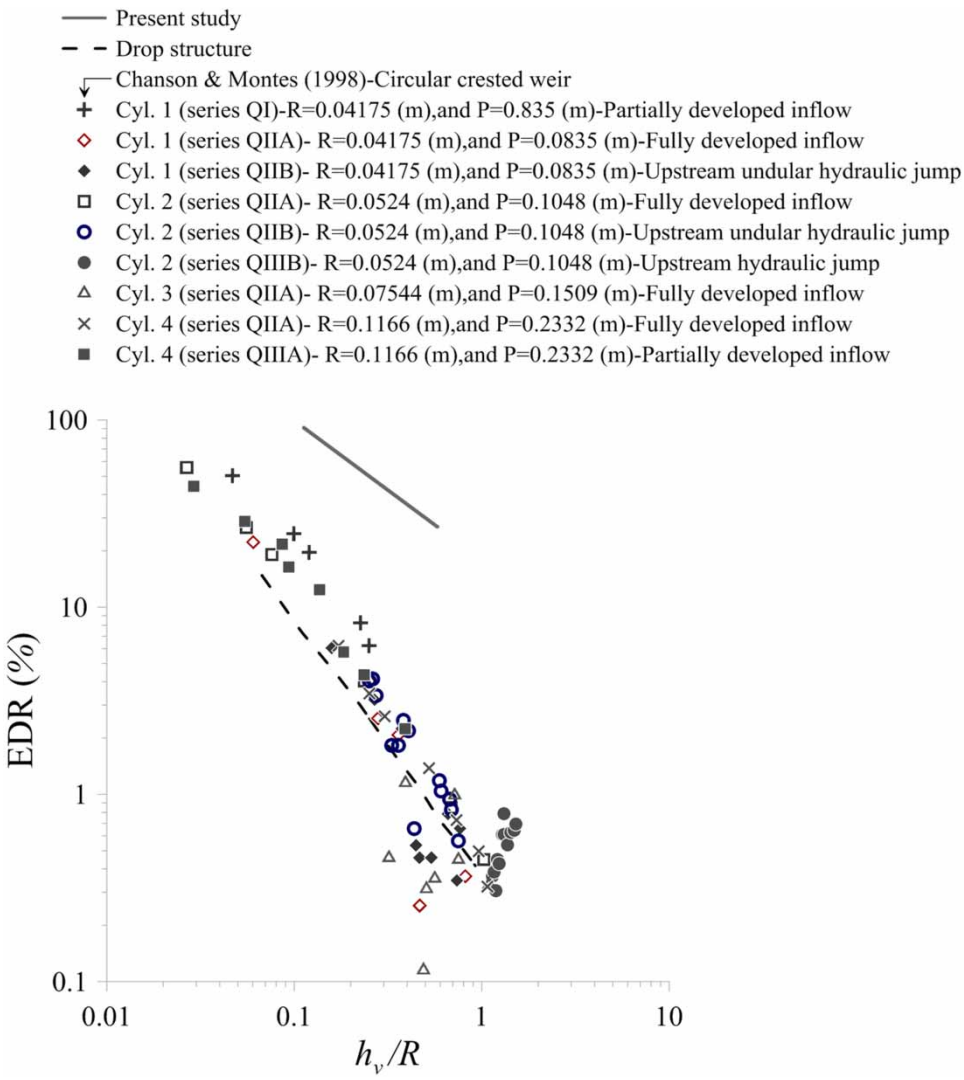

Figure 13 | Energy dissipation ratio of the inflatable weir, the circular-crested weir and the drop structure.

3.4. Horizontal length of the projectile-jet

One of the most important issues in inflatable weirs is the horizontal distance of the falling jet to the crest of the weir. The upstream head and geometry properties of an inflatable weir such as type of deflector and its angle of installation, angle of flow-jet take-off are involved in the horizontal length of the projectile-jet. The observed data of relative distance of projectile-jet (L_{impact}/R) versus the relative upstream head (h_V/R) in the presence of geometric properties of inflatable weir models, including α, ϕ_{def}, and θ are shown in Figure 14.

In inflatable weir overflow, if the nappe does not form or the flow sticks to the downstream part of the body of the weir, it will cause vibration in the body and turbulence of the flow at downstream. The purpose of installing the deflector on the body of the weir is to separate the overflowing nappe from the body of the weir and to prevent vibration of the body and flow turbulence. In experiments, nappe re-attachment was observed at an installation angle of 30° for low flow rates. The return of water to the body of the weir is an issue that is not approved. No nappe re-attachment was observed at an installation angle of 45 and 60°. The results also show that the length of the projectile-jet in the installation angle 45° is longer than the length of the projectile-jet in the other two installation angles. According to the analysis of the obtained results, it was found that α did not have much effect on the horizontal length of the projectile-jet and by fitting an equation to the data, the following equation was obtained:

$$\frac{L_{\text{impact}}}{R} = 4.81\left(\frac{h_v}{R}\right)^{0.21}(\phi_{def})^{-0.03}(\theta)^{-0.114} \tag{20}$$

where θ and ϕ_{def} are in degrees.

As can be seen from Figure 14, in the range of h_V/R between 0.2 and 0.6, by increasing the flow head, the length of the projectile-jet is greatly increased. For values of h_V/R more than 0.6, by an increasing head, the ascent rate of the length of the projectile-jet decreases sharply. Due to the supply of flow energy from upstream, with increasing the flow head, the amount of potential energy increases gradually and dominates over the kinetic energy. As a result, the rate of increasing the projectile-jet length will no longer be proportional to the increase of the flow head.

Figure 15 shows the trajectory jet curve obtained from the experimental data of this study (Equation (20)) and the theoretical relationship proposed by Chanson (1998). The increasing trend of projectile length in the inflatable weir follows the theoretical solution and the two graphs are matched by using the correction factor of 0.78.

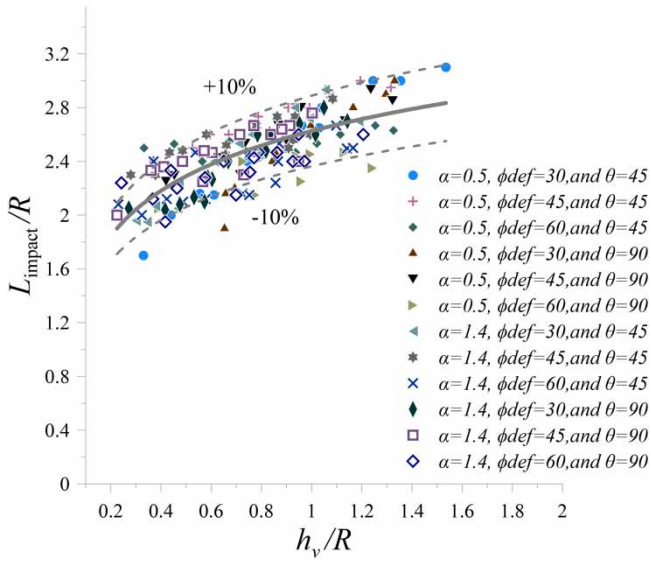

Figure 14 | Values of the length of the projectile in the inflatable weir against parameter the dimensionless of h_v/R.

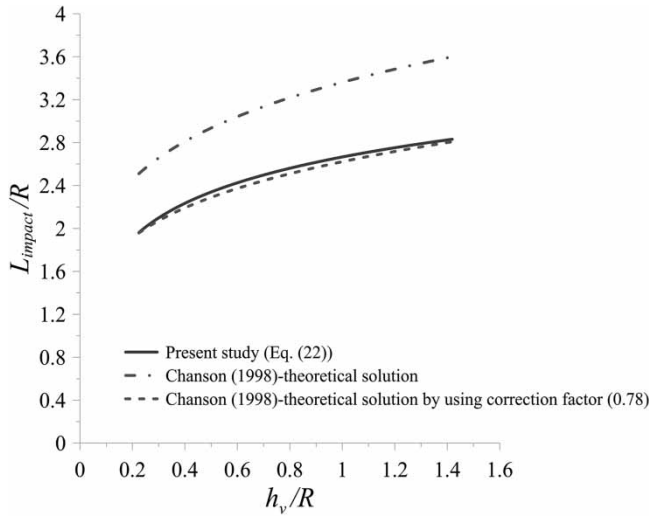

Figure 15 | Comparative curve of trajectory jet for inflatable weirs (experimental results and theorical solution).

3.5. Comparison and analysis of former equations by obtained results

In this section, the accuracy of the popular formulae presented by former scholars about estimating the discharge and the projectile-jet length are given. To this end, different error indexes (Equations (21)–(24)) were evaluated, and the results are shown in Table 3. The error for estimating the discharge by existing equations indicates that the high accuracy is related to the equation proposed by Al-shami (1983):

$$\mathrm{ME} = \frac{\sum_{i=1}^{N}(f_i - O_i)}{N} = \frac{\sum_{i=1}^{N} e_i}{N} \tag{21}$$

$$\mathrm{MAE} = \frac{\sum_{i=1}^{N}|f_i - O_i|}{N} = \frac{\sum_{i=1}^{N}|e_i|}{N} \tag{22}$$

$$\mathrm{MSE} = \frac{\sum_{i=1}^{N}(f_i - O_i)^2}{N} = \frac{\sum_{i=1}^{N} e_i^2}{N} \tag{23}$$

$$\mathrm{RMSE} = \sqrt{\frac{\sum_{i=1}^{N}(f_i - O_i)^2}{N}} = \sqrt{\frac{\sum_{i=1}^{N} e_i^2}{N}} \tag{24}$$

where f is the observed value, O is the calculated value by equations, e is the difference between the two observed and calculated values, and N is the total number of data.

Table 3 | Checking the other scholars' formulas accuracies

Equation		ME	RMSE	MSE	MAE
Q	Anwar (1967)	−0.0023	0.0029	8.59×10^{-6}	0.0023
	Al-Shami (1983) – Air filled	0.0022	0.0028	7.91×10^{-6}	0.0022
	Al-Shami (1983) – Water filled	0.0016	0.0019	3.73×10^{-6}	0.0016
	Alhamati *et al.* (2005b)	0.0016	0.0022	4.99×10^{-6}	0.0016
L_{impact}/R	Chanson (1998)	1.414	1.441	2.077	1.414

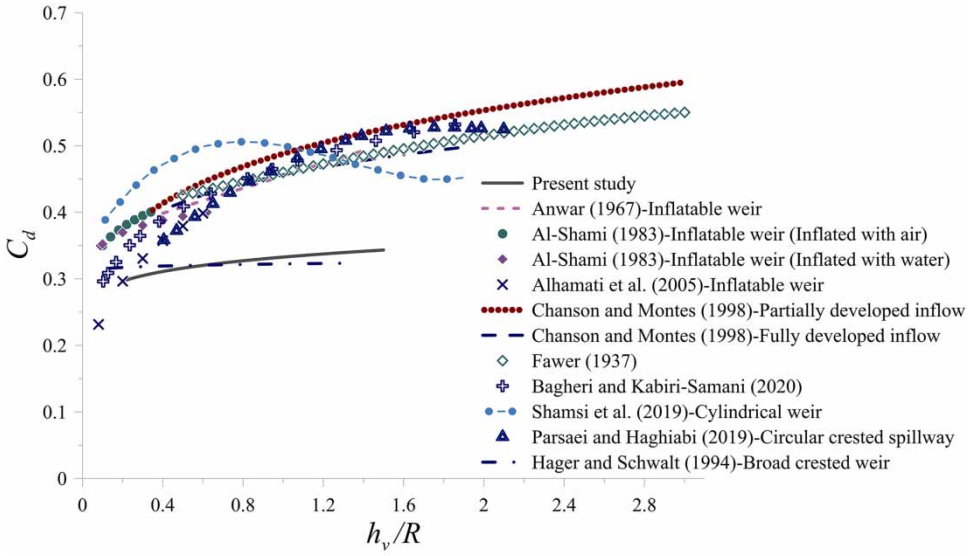

Figure 16 | Discharge coefficient versus h_V/R for inflatable, circular-crested, and broad-crested weir.

Figure 16 shows the discharge coefficient amounts given by Chanson & Montes (1998), Fawer (1937), and Bagheri & Kabiri-Samani (2020) for the circular crested weir, by Shamsi *et al.* (2019) for a cylindrical weir and by Hager & Schwalt (1994) for broad crested weir to compare with amounts for inflatable weirs. It should be noted that Equation (1) is used for broad crested weir and inflatable weir and Equation (25) is used for the circular crested weir to calculate the flow rate. The value $\left(2/3\sqrt{3}\right)$ is multiplied by the discharge coefficients of the circular crested weir for assimilation (Bos 1989):

$$q = \frac{2}{3}_{Cd}\sqrt{\frac{2}{3}}gh_V^{1.5} \tag{25}$$

R is half of the total height of the inflatable weir, half of the total height of the broad-crested weir is defined as R.

According to the experimental results and comparison with previous researches in Figure 16, it can be said that the discharge coefficient in the short-crested weirs and the circular-crested weir is higher than the broad-crested weir. The discharge coefficient in the inflatable weir is closed to the simple broad-crested weir at the low amount of h_V/R. The efficiency of inflatable weirs is increased more by increasing the amount of h_V/R in comparison to the simple broad-crested weir. The reason for the higher amount of discharge coefficient in circular-crested weir in comparison to the inflatable weir for the given range of h_V/R is the circular curve at the upstream of their body.

4. CONCLUSION

In this study the hydraulic properties of inflatable weirs included the profile of the water surface and jet profile leaving the deflector, discharge coefficient, and flow energy dissipation were investigated. The results are summarized as follow:

- The surface profile is smooth from upstream to downstream and no oscillating waves were seen.
- The discharge coefficient is independent of the angular position of the deflector on the body of the weir (ϕdef), the internal pressure coefficient (α), and the angle of the deflector's shape (θ), it means that these parameters do not have significant effects on the C_d; the most effective parameter on C_d is the ratio of (h_V/R).
- The shape of the deflector impacts on the energy dissipation. In fact, rectangular deflector models are more effective than triangular models; the inflatable weir can dissipate the energy of flow between 15 and 85% for the range of h_V/R between 0.7 and 0.1.
- There is a nappe re-attachment when the installation angle of the deflector is 30°. No nappe re-attachment was observed at an installation angle of 45 and 60°. The results also show that the length of the projectile-jet in the installation angle of 45° is longer than the length of the projectile-jet in the other two installation angles. The calculation of the horizontal length of the

projectile-jet showed that at low flow discharge, increasing the flow head greatly increases the length of the projectile-jet, and with further increase of the flow head, the projectile length is less affected by the head.

ACKNOWLEDGEMENTS

The authors thank Dr. AmirHamzeh Haghiabi (Lorestan University) for sharing his experiments about the laboratory modeling and studies of dams.

DATA AVAILABILITY STATEMENT

All relevant data are included in the paper or its Supplementary Information.

REFERENCES

Alhamati, A. A. N., Mohammed, T. A., Ghazali, A., Norzaie, J. & Al-Jumaily, K. K. 2005a Determination of coefficient of discharge for air-inflated dam using physical model. *Suranaree Journal of Science and Technology* **12** (1), 19–27.

Alhamati, A. A. N., Mohammed, T. A., Norzaie, J., Ghazali, A. H. & Al-Jumaily, K. K. 2005b Behavior of inflatable dams under hydrostatic conditions. *Suranaree Journal of Science and Technology* **12** (1), 1–18.

Al-Shami, A. 1983 *Theory and Design of Inflatable Structures*. University of Sheffield, Sheffield, UK.

Anwar, H. O. 1967 Inflatable dams. *Journal of the Hydraulics Division* **93** (3), 99–119.

Bagheri, S. & Kabiri-Samani, A. 2020 Overflow characteristics of streamlined weirs based on model experimentation. *Flow Measurement and Instrumentation*, **73**, 101720.

Bijankhan, M. & Ferro, V. 2017 Dimensional analysis and stage-discharge relationship for weirs: a review. *Journal of Agricultural Engineering* **48**, 1–11.

Bos, M. G. 1989 *Discharge Measurement Structures, Publication 20*. International Institute for Land Reclamation and Improvement/ILRI, Wageningen, The Netherlands.

Chanson, H. 1997 A review of the overflow of inflatable flexible membrane dams. *Australian Civil Engineering Transactions* **39** (2/3), 107.

Chanson, H. 1998 Hydraulics of rubber dam overflow: a simple design approach. In: *Proc., 13th Australasian Fluid Mechanics Conference*. Melbourne, Australia, pp. 255–258.

Chanson, H. & Montes, J. S. 1998 Overflow characteristics of circular weirs: effects of inflow conditions. *Journal of Irrigation and Drainage Engineering* **124** (3), 152–162.

Cheraghi-Shirazi, N., Kabiri-Samani, A. & Boroomand, B. 2014 Numerical analysis of rubber dams using fluid–structure interactions. *Flow Measurement and Instrumentation* **40**, 91–98.

Fawer, C. 1937 *Etude de quelques écoulements permanents à filets courbes*. *No. THESIS*.

Hager, W. H. & Schwalt, M. 1994 Broad-crested weir. *Journal of Irrigation and Drainage Engineering* **120** (1), 13–26.

Kumar, A. & ul-Islam, S. 2019 Inflation and deflation of rubber dam. In: Thomas, S., Rane, A. V., Kanny, K. & Dutta, A. (eds) *Plastics Design Library*. William Andrew Publishing, Norwich, pp. 67–98.

Parsaie, A. & Haghiabi, A. H. 2019 The hydraulic investigation of circular crested stepped spillway. *Flow Measurement and Instrumentation*, Elsevier, **70**, 101624.

Ramamurthy, A. S. & Vo, N.-D. 1993 Characteristics of circular-crested weir. *Journal of Hydraulic Engineering* **119** (9), 1055–1062.

Rand, W. 1955 Flow geometry at straight drop spillways. In: *Proceedings of the American Society of Civil Engineers*. ASCE, pp. 1–13.

Saleh, A. F. M. & Mondal, M. S. 2001 Performance evaluation of rubber dam projects of Bangladesh in irrigation development. *Irrigation and Drainage: The Journal of the International Commission on Irrigation and Drainage* **50** (3), 237–248.

Shamsi, Z., Parsaie, A. & Haghiabi, A. H. 2019 Optimum hydraulic design of cylindrical weirs. *ISH Journal of Hydraulic Engineering* **28**, 1–5.

Zheng, W., Band, S. S., Karami, H., Karimi, S., Samadianfard, S., Shadkani, S., Chau, K.-W. & Mosavi, A. H. 2021 Forecasting the discharge capacity of inflatable rubber dams using hybrid machine learning models. *Engineering Applications of Computational Fluid Mechanics*, **15** (1), 1761–1774.

First received 29 October 2021; accepted in revised form 20 February 2022. Available online 7 March 2022